

Local and global collapse pressure of longitudinally flawed pipes and cylindrical vessels

M. Staat*

Aachen University of Applied Sciences, Div. Jülich, Ginsterweg 1, 52428 Jülich, Germany

Abstract

Limit loads can be calculated with the finite element method (FEM) for any component, defect geometry, and loading. FEM suggests that published long crack limit formulae for axial defects under-estimate the burst pressure for internal surface defects in thick pipes while limit loads are not conservative for deep cracks and for pressure loaded crack-faces. Very deep cracks have a residual strength, which is modelled by a global collapse load. These observations are combined to derive new analytical local and global collapse loads. The global collapse loads are close to FEM limit analyses for all crack dimensions.

Keywords: Limit analysis; Global and local collapse; Axially cracked pipe; Pressure loaded crack-face

1. Introduction

Many burst tests with flawed pipes and vessels indicate that the burst pressure could be predicted by plastic limit analysis [1–3]. Limit load formulae are needed for defect assessment by the two criteria methods [4–8] or the engineering treatment method [9]. In the reference stress approach, they can be used to estimate nonlinear fracture mechanics parameters such as crack tip opening displacement (CTOD), J and C^* integrals [7,10].

Plastic limit loads for axial defects in pipes have been collected in Refs. [11,12]. A new type of local and global collapse loads has been derived in Ref. [13] combining the solutions for long defects and for slits. However, the formulae in Refs. [4,12,13] are not correct. Burst tests could be explained by limit analysis for a wide range of materials and of the dimensions of pipes and defects in Ref. [2]. However, Ref. [2] also showed that existing global collapse loads need to be further improved and proposed some ad hoc improvements. In Ref. [14], new global formulae have been obtained by approximation to incremental finite element limit analyses for thin pipes.

In this contribution, corrections of the thick pipe limit loads in Ref. [12] are made. They are then used to derive improved global and local collapse loads for thick pipes in the sense of Refs. [4,5,13]. The global collapse loads are compared to lower bound finite element limit loads with and without pressure loading on internal cracks. The results are used to suggest also new local collapse loads. In Ref. [3], the new global collapse loads are compared to 278 burst tests with thick and thin-walled pipes.

Reliable limit loads are important, because over-estimating burst pressure is clearly non-conservative. However, under-estimating limit loads could also be non-conservative, because it leads to under-predicting CTOD and crack opening area and consequently also to under-predicting leak rates.

1.1. Limit analysis

Stresses σ are admissible in a perfectly plastic material model, if they satisfy the Tresca or the von Mises yield condition $F(\sigma) \leq \sigma_y$. With equality $F(\sigma) = \sigma_y$ in one point, the elastic limit (0.2% strain limit) $\sigma_y = R_{p0.2}$ is assumed and yielding can begin there. In the context of the two-surface theory of plasticity, the yield surface $F_Y(\sigma) \leq \sigma_y = R_{p0.2}$ can harden kinematically within a bounding surface $F_U(\sigma) \leq \sigma_u$

* Tel.: +49 2461 99 3209; fax: +49 2461 99 3199.
E-mail address: m.staat@fh-aachen.de.

Nomenclature

a	crack length	$\bar{p}_{local}, p_{local}$	local collapse pressure old, new
c	crack depth	\bar{p}_L, p_L	collapse pressure of defect pipe old, new
D	constraint factor	R_1^*, R_1	distinction of crack-face loading old, new
E	Young's modulus	r_1, r_2	interior and exterior radius, respectively
eps	relative prognosis error	$R_{p0.2}$	0.2% proof stress
F_Y, F_U	yield function, bounding function	R_m	ultimate stress
f	function	t	wall thickness
M_{FL}	Folias factor	γ	limit load factor
M_1, M_2	Folias factor for internal and external defect	Ω	body
\mathbf{n}	exterior unit normal	$\partial\Omega_\sigma$	traction boundary
P	reference pressure	$\boldsymbol{\sigma}$	stress tensor
\bar{p}_0, p_0	burst pressure without defect old, new	σ_y	yield stress
$P_{exp}, P_{formula}$	experimental, predicted burst pressure	σ_u	ultimate stress
$\bar{p}_{global}, p_{global}$	global collapse pressure old, new	σ_F	flow stress

with some ultimate stress σ_u . In the simplest theory, the bounding surface is assumed as fixed in size, form, and location in stress space. Usually the same function is used for both surfaces, i.e. $F(\boldsymbol{\sigma}) = F_Y(\boldsymbol{\sigma}) = F_U(\boldsymbol{\sigma})$.

The structure Ω is loaded monotonically by the surface traction p on the traction boundary $\partial\Omega_\sigma$. For simplicity of the presentation, the body forces are neglected. The tractions are proportional to the internal pressure p . Starting from some reference pressure P , one may ask for the load factor $\gamma > 1$ by which P can be increased up to the collapse pressure $p_L = \gamma P$. The limit load p_L of a bounded kinematic hardening material can be computed exactly by the maximum problem, [15],

$$\begin{aligned} &\text{maximize } \gamma, \quad \text{such that } F(\boldsymbol{\sigma}) \leq \sigma_u \text{ in } \Omega, \\ &\quad -\text{div } \boldsymbol{\sigma} = \mathbf{0} \text{ in } \Omega, \quad \boldsymbol{\sigma} \mathbf{n} = \gamma P \mathbf{n} \text{ on } \partial\Omega_\sigma. \end{aligned} \quad (1)$$

The finite element discretisation of this optimization problem has been implemented in the finite element method (FEM) software PERMAS [16] and solved by a basis reduction technique. The numerical method of the limit analysis is presented in detail in Ref. [15]. The linear matching method has been developed from the elastic compensation method as an alternative for FEM limit

analysis [17]. Compared to the basis reduction method, the elastic compensation method is more easily programmed but it seems to have some difficulties to converge [18].

The maximum problem (1) shows that the burst pressure p_L is homogeneous of first order in σ_u . Therefore, one may write in non-dimensional similarity variables

$$\frac{p_L}{\sigma_u} = Df(a/t, a/c, t/r_1, r_2/r_1, \dots). \quad (2)$$

Here, the crack size is characterised by crack depth a and crack length $2c$ as shown in Fig. 1. The pipe geometry is characterised by r_1, r_2 and t which are internal and external radius and wall thickness. The constraint factor D distinguishes the yield condition

$$D = \begin{cases} 1 & \text{for Tresca,} \\ \frac{2}{\sqrt{3}} & \text{for von Mises} \end{cases} \quad (3)$$

for problems of pressurised pipes without defects.

Often the limit load analysis is only understood in a perfectly plastic context with $\sigma_u = \sigma_y = R_{p0.2}$ and the fictitious failure load is called the limit load. Eq. (1) shows that the yield stress has no influence for kinematic

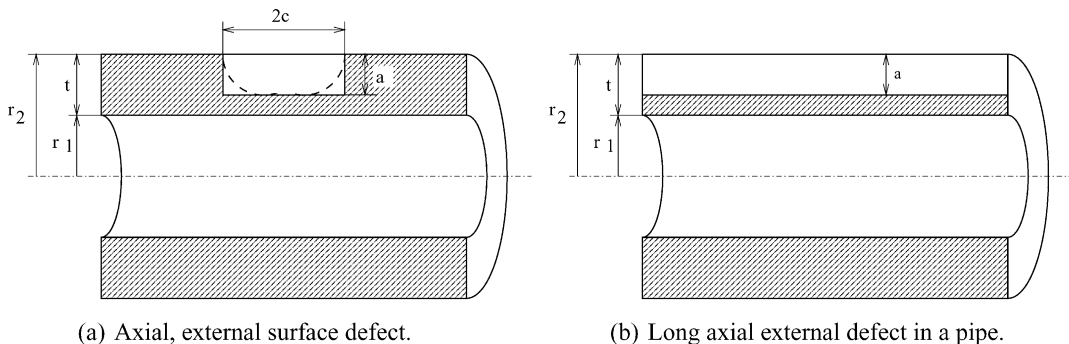


Fig. 1. External semi-elliptical surface defect and infinitely long defect in a pipe.

hardening material and that the actual load at failure is the ultimate load calculated with some σ_u . In the two criteria methods, only partial use is made of hardening by setting σ_u equal to the flow stress σ_F ,

$$\sigma_u = \sigma_F = \frac{R_{p0.2} + R_m}{2}. \quad (4)$$

In 300 burst tests with pipes with axial defects, this was a best choice [3]. Limit analysis predicts only global collapse load. The local collapse load is sometimes related with ligament (or net-section) collapse. As the ligament thickness tends to zero with $a \rightarrow t$, the local collapse load tends to zero. However, the pipe may still carry the limit load, i.e. the global collapse load.

2. The extreme cases

2.1. Thick pipe without defect

The burst pressure p_0 of the thick-walled pipe without defects is

$$\begin{aligned} \frac{p_0}{\sigma_u} &= D \ln \frac{r_2}{r_1} = D \ln \left(1 + \frac{t}{r_1} \right) \\ &= D \left[\frac{t}{r_1} - \frac{1}{2} \left(\frac{t}{r_1} \right)^2 + \frac{1}{3} \left(\frac{t}{r_1} \right)^3 - \dots \right], \end{aligned} \quad (5)$$

which must be assumed asymptotically by realistic limit load solutions for the cracked pipe. Therefore, the constraint factor D is introduced in all equations below, although it is originally omitted in most of the equations that have been cited from different references. The series expansion (5) converges for $t/r_1 \leq 1$. The solution for the Tresca yield function applies independently of the conditions at the pipe end. The solution for the hypothesis after von Mises does not apply to the open pipe with free ends.

The approximation

$$\frac{\bar{p}_0}{\sigma_u} = D \frac{t}{r_1} \quad (6)$$

for thin pipes over-estimates the load-carrying capacity of thick pipes, as the series expansion (5) shows. For $\nu=0.3$, the assumption of small deformations applies and therefore Eq. (5) remains valid with the Tresca hypothesis up to $r_2/r_1=5.43$ for closed ends [19]. The limits in which the relation is valid with the von Mises hypothesis are discussed in Ref. [19]. In the following, a closed pipe is assumed.

2.2. Pipes with penetrating axial cracks

For the collapse load of wall penetrating longitudinal cracks, semi-empirical formulae were set-up, which are often called Battelle formula or slit curve in the literature. According to Refs. [1,20], the burst pressure of

the penetrating axial crack can be written in the form

$$\frac{\bar{p}_L}{\sigma_u} = D \frac{t}{r_1 M_{FL}}. \quad (7)$$

A simple relation for the Folias factor M_{FL} is

$$M_{FL} = \sqrt{1 + 1.61 \frac{c^2}{r_1 t}}. \quad (8)$$

For $c \rightarrow 0$, $M_{FL} \rightarrow 1$. The burst pressure must then become the load (5) for the uncracked pipe. Therefore, it is suggested to generalise the Battelle formula (7) by

$$\frac{p_L}{\sigma_u} = \frac{D}{M_{FL}} \ln \frac{r_2}{r_1} \quad (9)$$

for thick pipes. This modification is supported by the FEM limit analyses for penetrating defects (i.e. $a/t=1$, most obviously for $a/c > 0.4$).

2.3. Long axial cracks in pipes

A lower bound for the limit load of a thick pipe with a long defect is obtained, if the pipe is divided into two coaxial pipes Pipe 1 carries the defect (slit pipe) and is stress free. Pipe 2 is a pipe thinned by a and is at yield in all of its points.

By this consideration, the collapse load

$$\lim_{c \rightarrow \infty} \frac{\bar{p}_L}{\sigma_u} = D \left[\left(\frac{r_1}{R_1^*} \right) \ln \left(\frac{r_2}{r_1 + a} \right) \right] \quad (10)$$

with

$$R_1^* = \begin{cases} r_1 & \text{pressure – excluding crack faces,} \\ r_1 + a & \text{pressure – including crack faces} \end{cases} \quad (11)$$

was presented for the internal crack with $R_1^* = r_1$ in Ref. [12]. That is a lower bound solution with a piecewise continuous effective stress field such that $F(\sigma(r)) = \sigma_u$ for $r_1 + a < r < r_2$. This incorrectly assumes that the internal pressure acts on a cylinder of radius $r_1 + a$. By correcting $r_1 + a$ to the internal pipe radius r_1

$$\lim_{c \rightarrow \infty} \frac{p_L}{\sigma_u} = D \left[\left(\frac{r_1}{R_1} \right) \left(\frac{r_1 + a}{r_1} \right) \ln \left(\frac{r_2}{r_1 + a} \right) \right] \quad (12)$$

equilibrium is achieved at least for the hoop stress. It is less conservative to replace R_1^* with R_1 ,

$$R_1 = \begin{cases} r_1 & \text{pressure – excluding crack faces,} \\ r_1 + \frac{a}{2} & \text{pressure – including crack faces.} \end{cases} \quad (13)$$

The limit load for the external defect

$$\lim_{c \rightarrow \infty} \frac{p_L}{\sigma_u} = D \ln \left(\frac{r_2 - a}{r_1} \right) \quad (14)$$

is correct in Ref. [12].

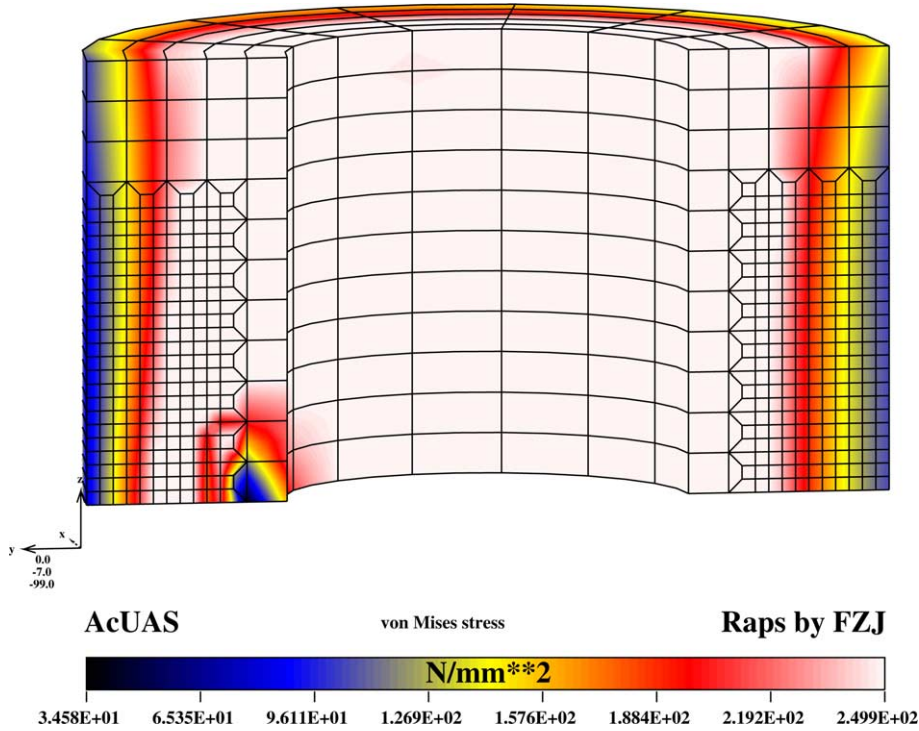


Fig. 2. FEM mesh and von Mises stress for internal defect in a thick pipe ($r_2/r_1=2$) with $\sigma_y=\sigma_u=250 \text{ N mm}^{-2}$. The defect causes unloading behind the crack front.

3. Global collapse of pipes containing axial surface defects

3.1. Global collapse of pipes containing internal defects

A lower bound of the global limit load dependent on the defect position is obtained, by dividing the pipe into two coaxial pipes, which together are in static equilibrium with the internal pressure [12]. Pipe 1 contains the surface crack as a penetrating defect. Pipe 2 is intact with a collapse load

after Eq. (5). In this way, the collapse load for the thick pipe with an internal axial surface crack has been obtained in Refs. [12,13]

$$\frac{\bar{p}_{\text{global}}}{\sigma_u} = D \left[\frac{a}{r_1 M_1} + \left(\frac{r_1}{R_1^*} \right) \ln \left(\frac{r_2}{r_1 + a} \right) \right] \quad (15)$$

with the Folias factor M_1

$$M_1 = \sqrt{1 + 1.61 \frac{c^2}{r_1 a}} \quad (16)$$

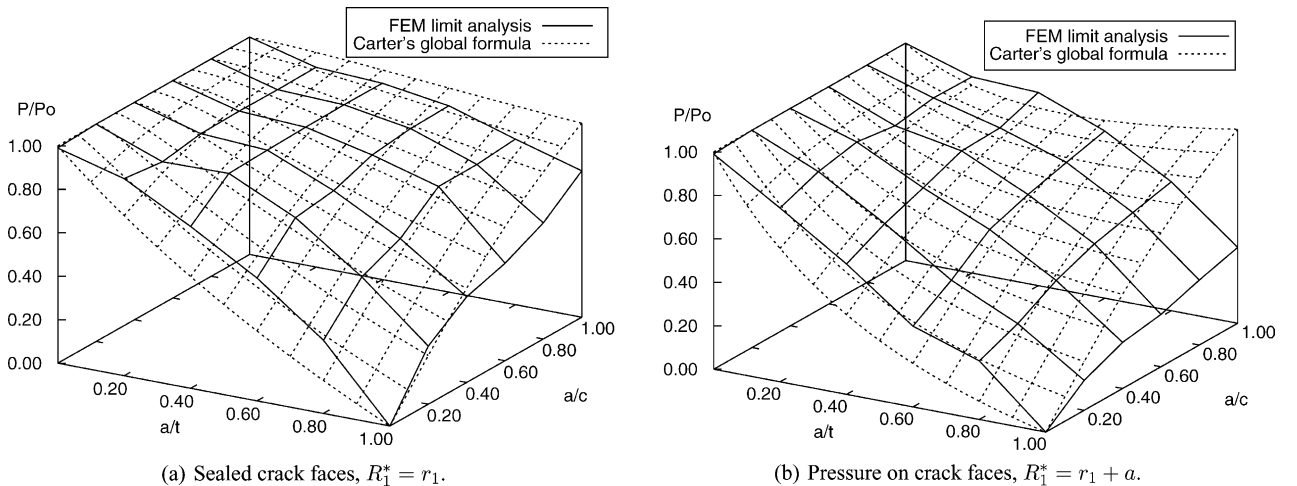


Fig. 3. Carter's global collapse pressure (\bar{p}_{global} , Eq. (15)) compared with FEM limit analyses for internal defects in a thick pipe with $r_2/r_1=2$. FEM —, formula \cdots . The pressures are normalised by p_0 .

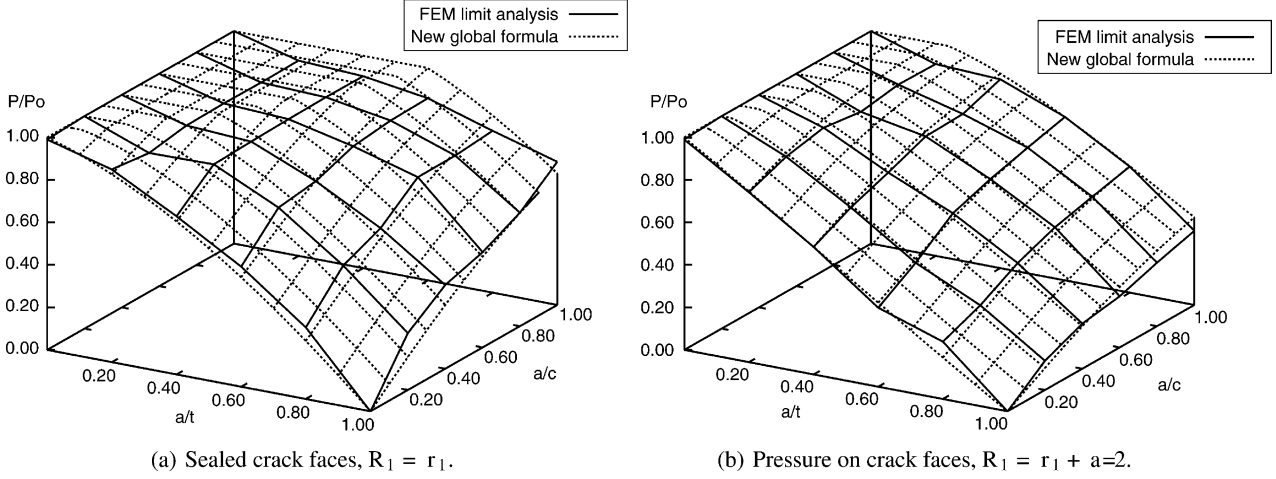


Fig. 4. New global collapse pressure (p_{global} , Eq. (17)) compared with FEM limit analyses for internal defects in a thick pipe with $r_2/r_1=2$. FEM —, formula The pressures are normalised by p_0 .

using Eqs. (7) and (10). R_1^* makes the distinction of cases of crack-face loading of Eq. (11) for the long defect part of the solution only.

The global collapse pressure is extensively checked against lower bound FEM limit analyses with rectangular and semi-elliptical defects. A typical FEM net of an internal defect in a thick-walled pipe with $r_2/r_1=2$ is shown in Fig. 2. Only one quarter of the pipe has been modelled, because of the symmetry of the problem. The rectangular defect causes unloading behind the crack front. There is no need for special crack tip elements or for mesh refinement, because of plastic collapse is not controlled by the crack tip. All analyses have been repeated with thin-walled pipes ($r_2/r_1=1.1$) with both types of crack shape, rectangular and semi-elliptical. These show similar trends but the differences between FEM limit analysis, old and new collapse formulae are less pronounced for thin pipes. The formulae have been derived for rectangular defects. Therefore, they are compared with FEM solutions for this crack shape.

The global collapse pressure (15), normalised with the burst pressure $p_0 = \sigma_u D \ln(r_2/r_1)$ of the pipe without a defect, is compared with FEM limit analyses in Fig. 3 for

a thick-walled pipe with $r_2/r_1=2$. The long crack limit (10), i.e. $c \rightarrow \infty$ or $a/c \rightarrow 0$, under-estimates the burst pressure. But the deep crack solution ($a/t > 0.8$) is not conservative for shorter defects with $a/c > 0.4$. Moreover, the pressure on the crack-faces is not considered for deep cracks such that the solution greatly over-estimates the burst pressure for all defect shapes a/c as is obvious from Fig. 3(b).

By use of the corrected Eqs. (9) and (12) an improved global collapse load is found

$$\frac{p_{\text{global}}}{\sigma_u} = D \min \left\{ \ln \left(\frac{r_2}{r_1} \right); \left(\frac{r_1}{R_1} \right) \left[\frac{1}{M_1} \ln \left(\frac{r_1 + a}{r_1} \right) + \left(\frac{r_1 + a}{r_1} \right) \ln \left(\frac{r_2}{r_1 + a} \right) \right] \right\}. \quad (17)$$

Here, the effect of pressure on the crack-faces is also correctly considered on the slit part of the solution. As limit value for $c \rightarrow \infty$ one obtains the new lower bound (12) for the local collapse because $M_1 \rightarrow \infty$.

Fig. 4 shows that Eq. (17) greatly improves the global collapse load for all limiting cases, for deep or long internal defects. The new long crack limit (12) is a close lower bound. For sealed crack-faces in Fig. 4(a), the solution

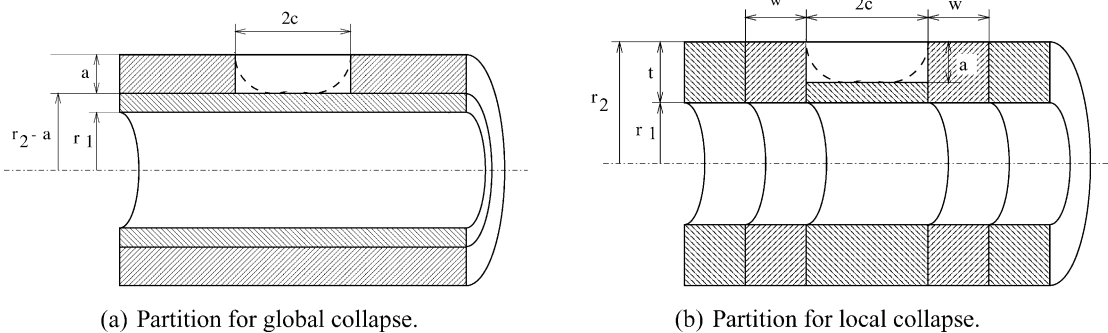


Fig. 5. Sections of different continuous stress fields at plastic collapse of an external axial surface crack in a pipe.

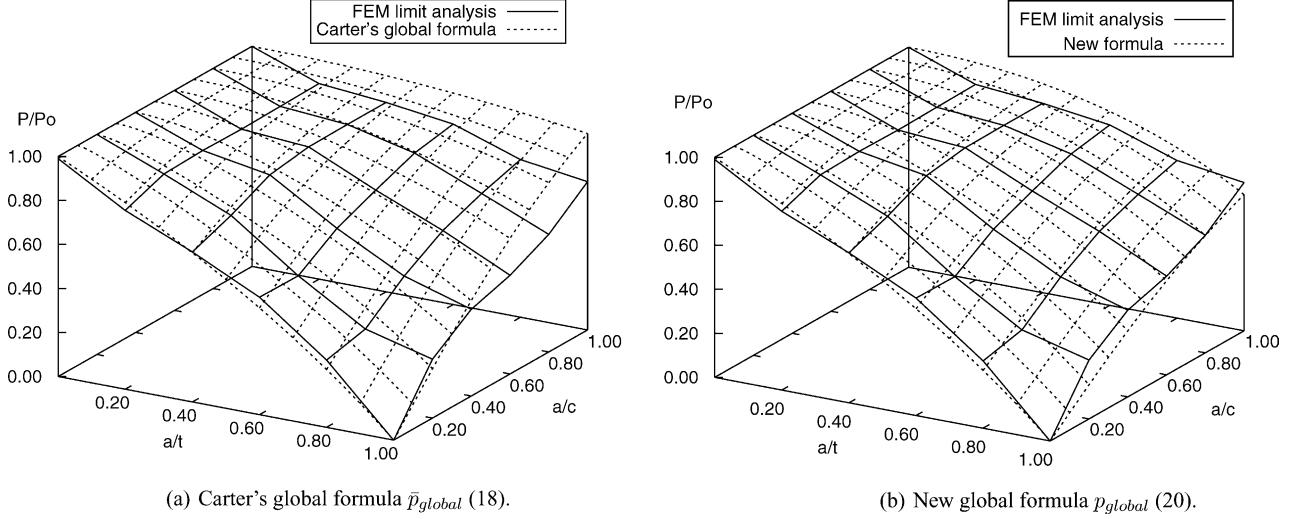


Fig. 6. Global collapse pressure formulae compared with FEM analyses for external defects in a thick pipe with $r_2/r_1=2$. FEM —, formula ···. The pressures are normalised by p_0 .

needs to be bounded by $p_0 = \sigma_u D \ln(r_2/r_1)$ for small defects. Fig. 4(b) shows that the new solution (17) is accurate for pressurised crack-faces for all parameters and that the limit p_0 hardly becomes active.

3.2. Global collapse of pipes containing external defects

In Refs. [4,13], the partition into sections as shown in Fig. 5(a) leads to a piecewise continuous stress field which has been used to derive global collapse loads for the thick pipe with an axial surface crack at the external wall

$$\frac{\bar{p}_{global}}{\sigma_u} = D \left[\frac{a}{(r_2 - a)M_2} + \ln\left(\frac{r_2 - a}{r_1}\right) \right] \quad (18)$$

with the Folias factor M_2

$$M_2 = \sqrt{1 + 1.61 \frac{c^2}{(r_2 - a)a}}. \quad (19)$$

This can be improved if Eq. (7) is replaced by Eq. (9) such that

$$\frac{\bar{p}_{global}}{\sigma_u} = D \left[\frac{1}{M_2} \ln\left(\frac{r_2}{r_2 - a}\right) + \ln\left(\frac{r_2 - a}{r_1}\right) \right]. \quad (20)$$

With finite c Eqs. (15) and (20) approach the solution (9) of the penetrating defect for $a \rightarrow t$. As limit value for $c \rightarrow \infty$, one obtains the lower bound of Eq. (12) for local collapse because $M_2 \rightarrow \infty$.

The modification of Eq. (18) in Eq. (20) concerns only the thick wall correction of the slit solution. The difference can be observed for the wall penetrating defect ($a/t=1$) in Fig. 6.

The new global formula (20) has been compared to 278 burst tests with external or penetrating defects in Ref. [3]. Fig. 7 shows that the relative prognosis error ϵ_{ps} ,

$$\epsilon_{ps} = \frac{P_{exp} - P_{formula}}{P_{formula}} \quad (21)$$

increases by its definition for long, deep defects due to uncertainties of geometric and material data ($\epsilon_{ps} \rightarrow \infty$ for $P_{formula} \rightarrow 0$ and $0 < P_{formula} < P_{exp}$; $\epsilon_{ps} \rightarrow -1$ for $P_{formula} \rightarrow 0$ and $P_{formula} > P_{exp} > 0$). Therefore, conservative data have to be used in defect assessment. Probabilistic fracture mechanics is a modern alternative [21].

All FEM limit analyses have been checked with internal and external semi-elliptical defects. Fig. 8 for external defects shows that the FEM limit analyses with rectangular defects are slightly conservative with respect to semi-elliptical defect shapes. The differences are smaller for thin pipes.

4. Local collapse of pipes containing axial surface defects

4.1. Local collapse of pipes containing internal defects

For the thick pipe with an internal semi-elliptical surface crack in the longitudinal direction local collapse loads are given¹ in Refs. [4,13]

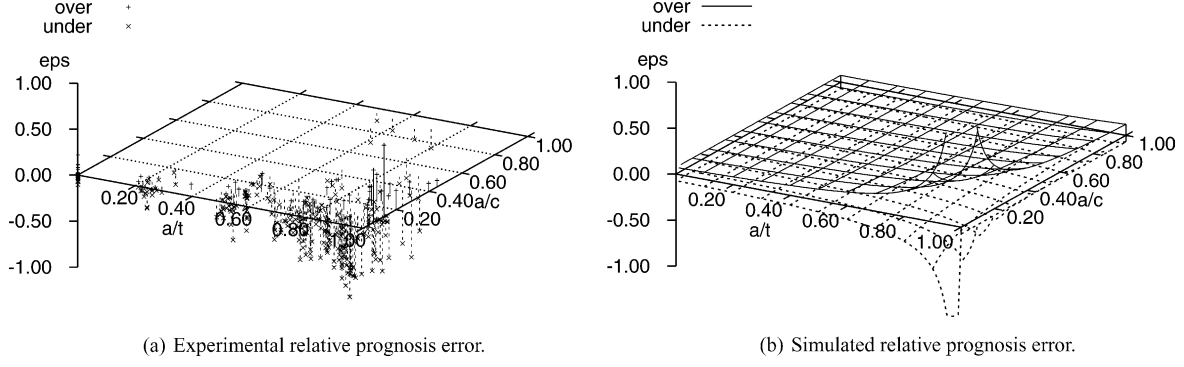
$$\frac{\bar{p}_{local}}{\sigma_u} = \frac{D}{s_1 + c} \left[s_1 \ln\left(\frac{r_2}{r_1}\right) + c \left(\frac{r_1}{R_1^*}\right) \ln\left(\frac{r_2}{r_1 + a}\right) \right] \quad (22)$$

along with

$$s_1 = \frac{ca(1 - \frac{a}{t})}{M_1 r_1 \left[\ln\left(\frac{r_2}{r_1}\right) - \left(\frac{r_1}{R_1^*}\right) \ln\left(\frac{r_2}{r_1 + a}\right) \right] - a} \quad (23)$$

and the distinction of cases of crack-face loading (11).

¹ A misprint in Ref. [4], p. AII.36, has been corrected in Eq. (22).



(a) Experimental relative prognosis error.

(b) Simulated relative prognosis error.

Fig. 7. Relative prognosis error of 278 experiments with external defects from Ref. [3] compared with $\pm 5\%$ variation of wall thickness t in the new global formula (20) plotted for a thick pipe ($r_2/r_1=2$): +, — burst pressure under-rated, \times , ... burst pressure over-rated.

Repeating all arguments that lead to the improved global limit load for the internal crack the modified local collapse load

$$\frac{p_{\text{local}}}{\sigma_u} = D \min \left\{ \ln \left(\frac{r_2}{r_1} \right); \frac{1}{S_1 + c} \left[S_1 \ln \left(\frac{r_2}{r_1} \right) + c \left(\frac{r_1 + a}{R_1} \right) \ln \left(\frac{r_2}{r_1 + a} \right) \right] \right\} \quad (24)$$

is obtained along with

$$S_1 = \frac{c \ln \left(\frac{r_1 + a}{r_1} \right) \left(1 - \frac{a}{t} \right)}{M_1 \left[\left(\frac{r_1}{R_1} \right) \ln \left(\frac{r_2}{r_1} \right) - \left(\frac{r_1 + a}{r_1} \right) \ln \left(\frac{r_2}{r_1 + a} \right) \right] - \ln \left(\frac{r_1 + a}{r_1} \right)} \quad (25)$$

and the distinction of cases (13). As limit value for $c \rightarrow \infty$ one finds (12).

No distinction can be made between global and local collapse for long defects with $c \rightarrow \infty$, i.e. $a/c \rightarrow 0$. Therefore, the local collapse can be checked against FEM limit analysis for this case. The new local formulae are close to the FEM solution whereas Carter's formulae are unnecessarily conservative for internal defects. A check against limit analysis is not possible for finite crack length. However, the local formulae are derived from the same extreme cases. Therefore, it is expected that all corrections of the solutions of these extreme cases will improve the local collapse pressures in the same way as it was proved for the global collapse. The same corrections as for the global collapse can be observed for the local collapse in Fig. 9. Also the local formulae (24) and (25) need to be bounded by p_0 . It is characteristic for the local collapse that there is no residual strength for wall penetrating defects ($a/t=1$). The largest difference between the new formulae (24) and (25) and the old local collapse pressure (22) and (23) is found for the pressure loaded defect. The more complete consideration of the pressure loading on the crack-faces in the new local formulae is considered more safe.

4.2. Local collapse of pipes containing external defects

The local collapse load for the external defect is derived in Ref. [13] from the piecewise continuous stress field with the partition into sections as shown in Fig. 5(b),

$$\frac{\bar{p}_{\text{local}}}{\sigma_u} = \frac{D}{S_2 + c} \left[s_2 \ln \left(\frac{r_2}{r_1} \right) + c \ln \left(\frac{r_2 - a}{r_1} \right) \right] \quad (26)$$

with

$$s_2 = \frac{ca \left(1 - \frac{a}{t} \right)}{M_2 (r_2 - a) \left[\ln \left(\frac{r_2}{r_1} \right) - \ln \left(\frac{r_2 - a}{r_1} \right) \right] - a} \quad (27)$$

By replacing Eq. (7) by Eq. (9) an improved solution

$$\frac{p_{\text{local}}}{\sigma_u} = \frac{D}{S_2 + c} \left[S_2 \ln \left(\frac{r_2}{r_1} \right) + c \ln \left(\frac{r_2 - a}{r_1} \right) \right] \quad (28)$$

is obtained with

$$S_2 = \frac{c \ln \left(\frac{r_2}{r_2 - a} \right) \left(1 - \frac{a}{t} \right)}{M_2 \left[\ln \left(\frac{r_2}{r_1} \right) - \ln \left(\frac{r_2 - a}{r_1} \right) \right] - \ln \left(\frac{r_2}{r_2 - a} \right)} \quad (29)$$

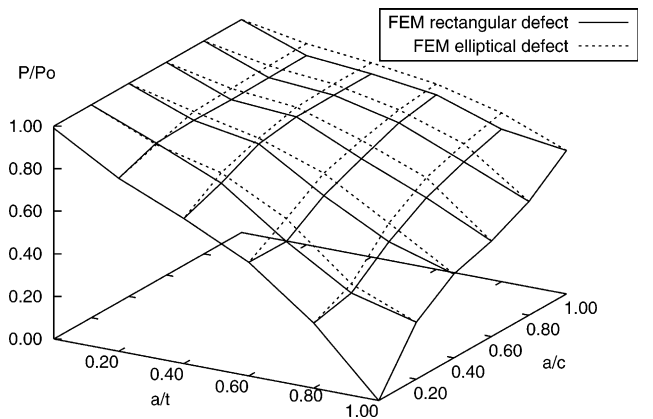


Fig. 8. FEM limit analyses for rectangular and semi-elliptical internal defects in a thick pipe ($r_2/r_1=2$). Rectangular —, semi-elliptical ... The pressures are normalised by p_0 .

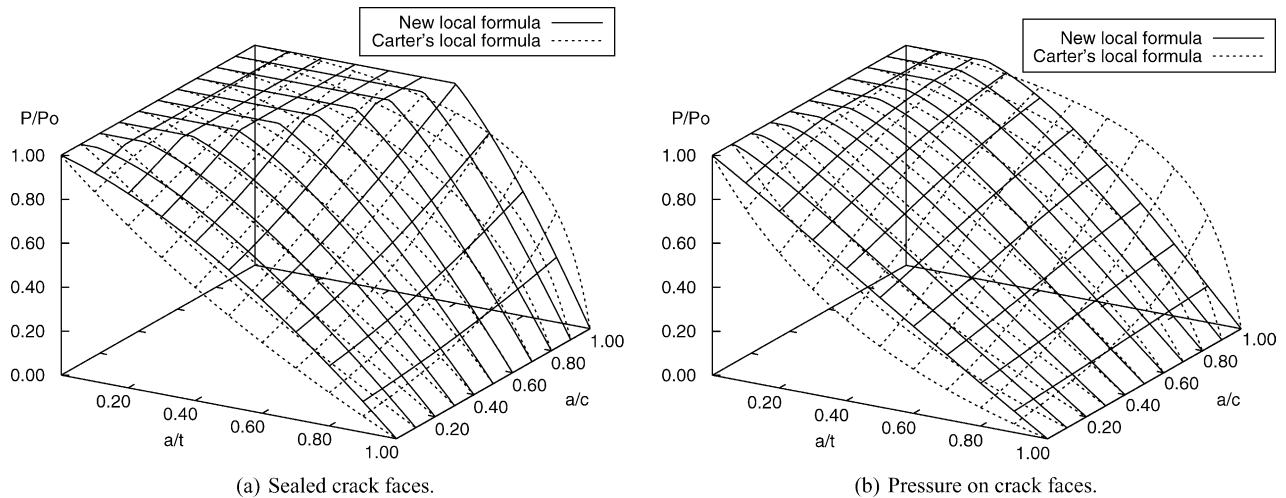


Fig. 9. New local collapse pressure (p_{local} , Eqs. (24) and (25)) compared with Carter's local collapse pressure (\bar{p}_{local} , Eqs. (22) and (23)) for internal defects in a thick pipe with $r_2/r_1=2$. New formula —, Carter's formula \cdots . The pressures are normalised by p_0 .

One finds Eq. (14) as the limit function for $c \rightarrow \infty$. The new and the old local collapse formulae (28), (29) and (26), (27), respectively, are compared in Fig. 10.

5. Conclusions and comments

A new close lower bound limit load has been derived for internal long defects in thick-walled pipes. It replaces a widely used but strongly conservative limit load. The slit solution for fully penetrating cracks in thin pipes has been modified for thick pipes. The effect of pressure loading of crack-faces has been reconsidered.

Improved global and local collapse loads have been proposed for internal and external axial defects for all cases: long, short (to defect free) or deep (including penetrating) cracks, thin and thick pipes. The new formulae are

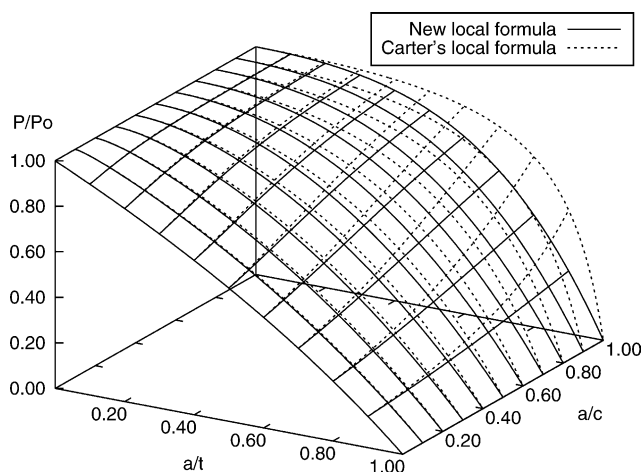


Fig. 10. New local collapse pressure (p_{local} , Eqs. (28) and (29)) compared with Carter's local collapse pressure (\bar{p}_{local} , Eqs. (26) and (27)) for external defects in a thick pipe with $r_2/r_1=2$. New formula —, Carter's formula \cdots . The pressures are normalised by p_0 .

particularly recommended as safe global and local solutions for crack-faces with applied pressure, because previously existing solutions are found to severely over-estimate the residual strength for shorter cracks.

The new global collapse loads have been checked against lower bound finite element (FEM) limit analyses with rectangular defects in thick pipes (wall thickness equal to internal radius). Additional FEM checks have been made with semi-elliptical defects and for thin-walled pipes.

Acknowledgements

The lower bound limit analyses with the PERMAS FEM code and a basis reduction method have been performed by Y. Qesmi as part of his Diploma Thesis. M. Bessi has checked the analyses with semi-elliptical defects in his Diploma Thesis.

References

- [1] Kiefner JF, Maxey WA, Eiber RJ, Duffy AR. Failure stress loads of flaws in pressurized cylinders, vol. 536. Philadelphia: ASTM STP; 1973 p. 461–81.
- [2] Staat M, Szelinski E, Heitzer M. Kollapsanalyse von längsfehlerbehafteten Rohren und Behältern unter Innendruck. 27. MPA-Seminar, Stuttgart, October 4–5; 2001.
- [3] Staat M. Plastic collapse analysis of longitudinally flawed pipes and vessels. Nucl Eng Des 2004 in press (doi: 10.1016/j.nucengdes.2004.08.002).
- [4] Al-Laham S. Stress intensity factor and limit load handbook. British Energy Report EPD/GEN/REP/0316/98, Gloucester, UK; 1999: Issue 2 [also in Ref. [5]].
- [5] Bannister AC, Webster SE. S.I.N.T.A.P. Procedure and background documents. Version 1b. Rotherham, UK: Corus Group plc.; 2002.
- [6] Andersson P, Bergman M, Brickstad B, Dahlberg L, Nilsson F, Sattari-Far I. A procedure for safety assessment of components with cracks—handbook. SAQ/FoU-Report 96/08, Stockholm: SAQ Kontroll AB; 1996.

- [7] R6: assessment of the integrity of structures containing defects. British Energy, Gloucester, UK, Rev. 4; 2001.
- [8] Ainsworth RA. Foreword: special issue on flaw assessment methods. *Int J Pressure Vessels Piping* 2000;77:853.
- [9] Schwalbe K-H, Zerbst U. The engineering treatment method. *Int J Pressure Vessels Piping* 2000;77:905–18.
- [10] R5: an assessment procedure for the high temperature response of structures. British Energy, Issue 3, Gloucester, UK; 2003.
- [11] Görner F, Munz D. Plastische Instabilität. In: Munz D, editor. *Leckvor-Bruch-Verhalten druckbeaufschlagter Komponenten*. Fortschr. Ber. VDI-Z. Reihe 18, Nr.14. Düsseldorf: VDI; 1984.
- [12] Miller AG. Review of limit loads of structures containing defects. *Int J Pressure Vessels Piping* 1988;32:197–327.
- [13] Carter A.J. A library of limit loads for FRACTURE.TWO. Nuclear Electric, Internal Report TD/SID/REP/0191; 1991/92
- [14] Kim Y-J, Shim D-J, Huh N-S, Kim Y-J. Plastic limit pressures for cracked pipes using finite element limit analysis. *Int J Pressure Vessels Piping* 2002;79(5):321–30.
- [15] Heitzer M, Staat M. Basis reduction technique for limit and shakedown problems. In: Staat M, Heitzer M, editors. *Numerical methods for limit and shakedown analysis—deterministic and probabilistic problems*. NIC-Series, vol. 15. Jülich: John von Neumann Institute for Computing; 2003 <http://www.fz-juelich.de/nic-series/volume15/nic-series-band15.pdf>.
- [16] PERMAS user's reference manual. PERMAS version 8.0, Stuttgart: INTES Publication No. 450, Rev. F; 2000.
- [17] Chen HF, Ponter ARS. Shakedown and limit analyses for 3-D structures using the linear matching method. *Int J Pressure Vessels Piping* 2001;78:443–51.
- [18] Staat M, Schwartz M, Lang H, Wirtz K, Heitzer M. Design by analysis of pressure components by non-linear optimization. In: Zeman JL, editor. *Pressure vessel technology 2003*. Proceedings ICPVT-10, July 7–10, 2003, Vienna, Austria.
- [19] Chakrabarty J. *Theory of plasticity*. New York: McGraw-Hill; 1987.
- [20] Hahn GT, Sarrate M, Rosenfeld AR. Criteria for crack extension in cylindrical pressure vessels. *Int J Fract Mech* 1969;5:187–210.
- [21] Staat M. Reliability of an HTR-module primary circuit pressure boundary: influences, sensitivity, and comparison with a PWR. *Nucl Eng Des* 1995;158:333–40.